Xiao-Xu Shi[1]
Liang Xu[1]
Hong-Quan Duan[1,2]
Yan-Ping Huang[1,2]*
Zhao-Sheng Liu[1,2]

[1]College of Pharmacy, Tianjin Medical University, Tianjin, P. R. China
[2]Basic Medical Research Centre of Tianjin, Tianjin Medical University, Tianjin, P. R. China

Received October 4, 2010
Revised January 19, 2011
Accepted January 19, 2011

Research Article

CEC separation of ofloxacin enantiomers using imprinted microparticles prepared in molecular crowding conditions

Molecular crowding is a new concept to obtain molecularly imprinted polymers (MIPs) with greater capacity and selectivity, which could shift the equilibrium of a print molecule reacting with functional monomers in the direction of complex formation side. In this work, molecular crowding agent was first applied to the preparation of MIPs microparticles by precipitation polymerization. A new system of molecular crowding surrounding was developed, composed of polystyrene and tetrahydrofuran, in the presence of the template (*S*)-ofloxacin. Partial filling capillary electrochromatography (CEC) was utilized to evaluate imprinting effect of the resulting microparticles by chiral separations of ofloxacin. Some important parameters in the preparation, i.e. template to monomer ratio, influence of cross-linking monomers and functional monomer composition on the CEC separation of MIP microparticles were investigated. Baseline separation of ofloxacin ($R_s = 1.53$) was obtained under optimized conditions and the highest theory plate of the later eluent (*S*)-ofloxacin was 5400. The textural and morphological parameters for imprinted particles, such as Brunauer–Emmett–Teller surface areas, pore volumes and pore size distributions have also been determined. Compared to the MIP microparticle prepared by conventional precipitation polymerization, the (*S*)-ofloxacin-imprinted particles formed under molecular crowding conditions showed higher selectivity ($\alpha = 1.09$) and separation efficiency (< 25 min) in the CEC mode.

Keywords:
CEC / Crowding agent / Microparticle / Molecularly imprinted polymer / Ofloxacin
DOI 10.1002/elps.201000515

1 Introduction

Molecular imprinting is a state-of-the-art technique by which specific recognition sites are constructed in a polymer matrix in the presence of a template molecule [1, 2]. After the removal of the template from the resultant molecularly imprinted polymer (MIP), 3-D cavities with ''memory'' for the used template molecule are left. The advantages that MIPs possess over biopolymers are low cost and good physical and chemical stability. Due to remarkable selectivities, MIPs have found application in enzyme-like catalysis [3], biomimetic sensors [4], antibody mimics [5], solid-phase extraction [6], drug delivery systems [7] and chromatography [8].

Molecular imprinting involves arranging polymerizable functional monomers around a print molecule. This is achieved by utilizing either noncovalent interactions such as hydrogen bonding, ion-pair interactions, etc. (noncovalent imprinting) or reversible covalent interactions (covalent imprinting) between the print molecule and the functional monomers. While the well-defined stoichiometry associated with the covalent approach certainly has its merits, noncovalent imprinting and recognition versatile technique for the generation of synthetic techniques are dominated in the literature, as they facilitate readily adaptable and rapid synthesis, close resemblance to the molecular recognition mechanisms of natural receptors and the availability of substantial functional monomer libraries reported in the literature.

Correspondence: Dr. Zhao-Sheng Liu, College of Pharmacy, Tianjin Medical University, Tianjin 300070, P. R. China
E-mail: zhaoshengliu@sohu.com
Fax: +086-022-23536746

Abbreviations: **AM,** acrylamide; **BET,** Brunauer–Emmett–Teller; **BMA,** butyl methacrylate; **DVB,** divinylbenzene; **EDMA,** ethylene glycol dimethacrylate; **MAA,** methacrylic acid; **MIP,** molecularly imprinted polymer; **γ-MPS,** 3-trimethoxysilylpropyl methacrylate; **PS,** polystyrene; **TRIM,** trimethylolpropane trimethacrylate; **4-VP,** 4-vinyl pyridine

*Additional corresponding author: Dr. Yan-Ping Huang
E-mail: huangyp100@163.com

Colour online: See the article online to view Fig. 3 in colour.

For MIPs created by noncovalent imprinting, monomers that can undergo noncovalent interactions are brought together with the template molecule and the cross-linking agent to form well-defined complexes of template and monomer. Whether molecular imprinting succeeds or not depends critically on the efficiency of complexation between the print molecule and the functional monomers; thus, the achievable selectivity of resultant MIPs is governed by the nature and stability of these complexes. However, the noncovalent imprinting technique is still useful only in limited cases due to a lack of generic procedures for obtaining stable complexes in pre-polymerization mixtures. Therefore, efforts have been found on stabilizing the complex and increasing imprinting efficiency, including selection of suitable functional monomers with computer-aided rational approaches [9] and optimization of the polymerization temperature [10] and solvent in stabilizing the complex [11]. In addition, high pressure has also been examined as a means of stabilizing the complexes and resulted in higher specificity [12]. However, a new, generally applicable approach for stabilizing the complex is still required.

As an important feature of the molecular environments in biological cells, recent studies [13–15] have shown that molecular crowding in biological cells affects the stability of higher order structures of biopolymers and promotes the association of biomolecules. In the case of molecular imprinting, molecular crowding could shift the equilibrium of a print molecule reacting with functional monomers in the direction of complex formation side. Recently, Matsui et al. [16] demonstrated that the intermolecular interactions between the template molecule and functional monomers are stabilized by molecular crowding. Higher retention and selectivity can be found on the crowding-based MIPs than non-crowding-based MIPs. This suggested that molecular crowding is a powerful approach to producing artificial receptors with greater capacity and selectivity. However, for a chiral stationary for high-performance liquid chromatography (HPLC), the MIP prepared with molecular crowding indicates low column efficiency (S.-J. Zhang et al, paper submitted) [16] and more efforts need to be done.

Capillary electrochromatography (CEC) is a hybrid method that combines the advantage of the high separation efficiency of CE and the various retention mechanisms and selectivity offered by HPLC. In CEC, EOF is formed across the entire column and results in an almost flat profile. Therefore, higher column efficiency can be obtained for CEC-based MIP separations [17–20]. Furthermore, many formats of MIP can be used in CEC analysis, including monolithic column [21–23], open tubular capillary [24–27] and particle-based technique [28–37]. For example, using the partial-filling technique, MIP microparticles can be used as additive in the background electrolyte [31–37] for CEC and has been shown to have higher efficiency on enantiomeric separation.

The present work reports a new strategy to prepare MIP microparticles by precipitation polymerization, which is conducted in a surrounding of a crowding-inducing agent (Fig. 1). Precipitation polymerization is a methodology to prepare submicrometer MIP particle [38]. The resulting MIP microparticles are produced from a dilute monomer solution and can be used in CEC mode by partial-filling technique. The small amount of pseudostationary phase needed to perform separations on a CE system makes the cost of the pseudostationary phase a less important problem. Furthermore, the composition and concentration of the MIP is easy to change from run to run, which facilitates rapid optimization. In this study, polystyrene (PS) was chosen to be the crowding agent and dissolved in tetrahydrofuran (THF) (used as porogenic agent in this experiment). Ofloxacin was selected as template since the separation of ofloxacin enantiomers has attracted many interests from analytical scientists [39–46]. The imprinting effect in this new polymerization system was evaluated by the ability of chiral separation provided with microparticle MIPs. Important parameters such as the choice of solvents and cosolvents, template to monomer ratio, the type of cross-linking monomers and functional monomer composition have been investigated for arriving at the right size and morphology.

2 Materials and methods

2.1 Chemicals

S-ofloxacin and *rac*-ofloxacin were obtained from Sigma (St. Louis, MO, USA). Methacrylic acid (MAA) was from Chengdu Jinshan Chemical Reagent (Chengdu, China). Butyl methacrylate (BMA) and divinylbenzene (DVB) were obtained from Tianjin Bodi Chemical (Tianjin, China). Ethylene glycol dimethacrylate (EDMA), trimethylolpropane trimethacrylate (TRIM), 4-vinyl pyridine (4-VP) and PS were purchased from Aldrich. 3-Trimethoxysilylpropyl methacrylate (γ-MPS) was from Acros (Geel, Belgium). Acrylamide (AM) was purchased from Beijing Pubo biotech (Beijing, China). 2, 2′-Azobis (2-isobutyronitrile) (AIBN) was supplied by Special Chemical Reagent Factory of Nankai University (Tianjin, China). ACN (HPLC grade) was from Fisher (New Jersey, USA). Other analytical reagents were from Tianjin Chemical Reagent (Tianjin, China). Fused-silica capillaries with 100 μm id and 375 μm od were purchased from Xinnuo Optic Fiber Plant (Hebei, China).

2.2 Preparation of molecularly imprinted microparticles

The template molecule, (*S*)-ofloxacin, the radical initiator (AIBN), functional monomers (MAA) and cross-linking monomers (EDMA) were dissolved in PS-THF (40 mg/mL) in a round-bottom flask in proportions stated in Table 1. The pre-polymerization mixture was sonicated for 15 min followed by degassing by a stream of nitrogen for 3 min. The flask was sealed and put into a water bath and heated at 53°C. After completed polymerization, the fraction of MIP

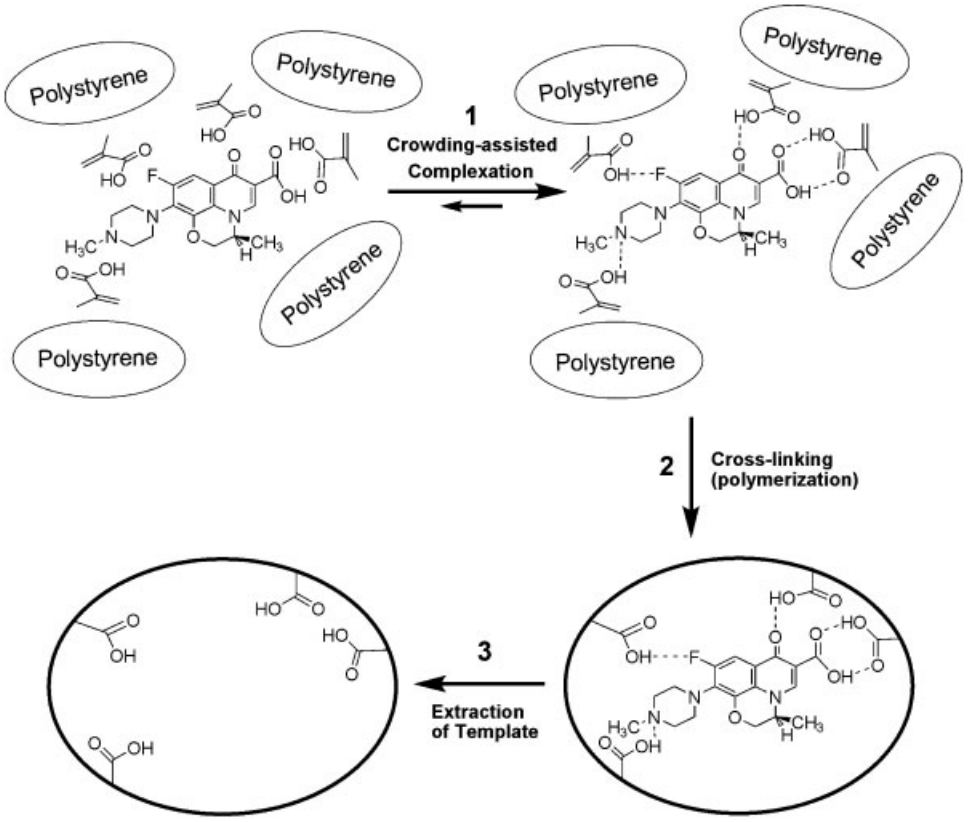

Figure 1. Schematic representation of molecular imprinting under molecular crowding conditions. (*S*)-ofloxacin (a template molecule) is mixed with MAA (a functional monomer) in THF with PS as a macromolecular co-solute (1); cross-linking with EDMA is achieved by heating, forming a three-dimensional polymer matrix (2); template is extracted from the matrix to leave behind a binding site (3).

Table 1. Recipes of preparation and textural parameters for (S)-ofloxacin-imprinted microparticles

Polymer	Template (mmol/L)	Functional monomers (mmol/L)				Cross-linkers (mmol/L)		Size (nm)	S_{BET} (m^2/g)	S_t (m^2/g)	V_p (10^{-3} cm^3/g)	D_{mean}(nm)
		MAA	BMA	AM	4-VP	EDMA	TRIM					
MIP A	0.08	0.32				1.6		721 ± 91	3.3	4.9	1.99	4.89
MIP B	0.053	0.32				1.6		996 ± 133	2.3	3.6	1.43	4.69
MIP C	0.107	0.32				1.6		2090 ± 299	4.8	4.5	1.94	8.18
MIP D	0.08	0.16	0.16			1.6		1470 ± 241	5.6	7.8	2.42	4.85
MIP E	0.08	0.32					0.64	783 ± 117	3.4	4.9	0.73	5.45
MIP F	0.08	0.32					0.96	1320 ± 190	3.3	4.9	N.R.	N. R.
MIP G	0.08	0.32				1.6		775 ± 92	128	106.9	453.7	16.84
MIP H	0.08	0.32				1.6		> 3700	12.3	13.7	19.03	11.18
MIP I	0.08	0.16			0.16	1.6		528 ± 62				
MIP J	0.08	0.16		0.16		1.6		> 3600				
MIP K	0.08	0.24	0.08			1.6		2539 ± 803				
MIP L	0.08	0.08	0.24			1.6		2606 ± 811				
MIP M	0.08	0.32					0.32	> 14 000				
NIP A	–	0.32				1.6		611 ± 63	2.4	3.3	0.64	5.35
NIP G	–	0.32				1.6		473 ± 42	17.6	18.4	32.99	16.37

S_{BET}: BET area; S_t: *t*-plot external surface area; V_p: cumulative volume of pores; D_{mean}: average pore diameter. A–F and I–M were prepared using PS-THF; G and H were prepared using ACN and chloroform as solvent, respectively.

microparticles was separated from the suspension. The two fractions were washed by successive centrifugation (14 500 rpm for 15 min) and resuspension (sonication for 15 min) twice in methanol:acetic acid (70:30, v/v) and once in ACN. Finally, the polymer particles were dried and stored at room temperature until use.

2.3 CEC

Since the migration of the MIP plug is partially determined by the EOF, a derivatized capillary with reduced EOF was used in order to be able to use a MIP plug of appropriate length and still have the analyte to reach the detection

window prior to the MIP. In this study, a fused-silica capillary was derivatized with γ-MPS. The derivatization was performed by successively rinsing the capillary for 2 h with 1 mol/L NaOH, water, 0.1 mol/L HCl and water, followed by drying with a stream of nitrogen gas. The capillary was then rinsed and filled with a solution of toluene/γ-MPS (85:15, v/v). This solution was kept in the capillary overnight and finally the capillary was rinsed with toluene and dried.

CEC experiments were carried out on a K1050 system (Kaiao, Beijing, China) equipped with a UV detector. A Lenovo personal computer with CXTH-3000 software for CE was used. The electrolyte was composed of ACN/10 mmol/L, pH 5.0, and acetate–sodium acetate buffer solution (90:10, v/v). MIP micro particles were suspended in the electrolyte to 5 g/L. The samples were prepared from 10 mmol/L water solutions diluted with electrolyte to give samples of 10 μmol/L concentration. Water-based buffers were filtered using 0.2-μm microporous filtering film. All solutions were degassed by sonication. A γ-MPS-derivatized capillary (47.5 cm total length; 37.5 cm effective length) was used in CEC separation. Prior to the first CEC analysis every day, the capillary was rinsed with water and electrolyte for 15 min each. Between consecutive runs, the capillary was rinsed with electrolyte for 5 min. The MIP microparticle suspensions and the samples were introduced hydrodynamically at 15 mbar for 6.0 s and 4.0 s, respectively. The separation voltage was 5 kV. UV detection was performed at 254 nm.

In this paper, separation factor is evaluated using α, which is calculated by [47]

$$\alpha = t_2/t_1$$

because some of analytes are eluted prior EOF; t_1 and t_2 are the retention times of the first and second peaks.

The degree of enantiomer separation was represented by a normalized separation index $\Delta t_R/t_{R1}$, where Δt_R is the difference in the elution times of the enantiomers at peak maximum and t_{R1} is the retention time of the first eluted enantiomer.

2.4 Characterization of the MIP microparticles

Scanning electron microscopy (SEM) was used for the characterization of MIP particles. The MIP particles samples were dispersed on glass slide and cemented into aluminum SEM planchets. Samples were sputter-coated with gold before obtaining images. All SEM images were obtained using a Shimadzu SS-550 scanning electron microscope, operated at 15 kV and a filament current of 60 mA.

All of the particles were dispersed and diluted into methanol, and the particle sizes were determined by Zetasizer Nano ZS (Malvern Instrument, UK). Diversity of size distributions and volume weighted mean diameters were obtained as shown in Table 1.

2.5 Gas adsorption experiments

Brunauer–Emmett–Teller (BET) surface areas and the porosity of the MIP particles were measured at 77 K by nitrogen adsorption–desorption isotherms using a Micromeritics ASAP 2020 Surface Area and Porosity Analyzer (Micromeritics Instrument, Norcross, GA, USA). Samples were vacuum degassing (10^{-3} Torr) at 60°C for 4 h before the adsorption experiments. The Barret–Joyner–Halenda (BJH) method was used for calculating the pore size distribution. Kelvin equation was also used to calculate porosity and pore size distribution. Values of the BET area (S_{BET}), *t*-plot external surface area (S_t), cumulative volume of pores between 1.70 and 50.00 nm diameter (V_p) and average pore diameter (D_{mean}) are displayed in Table 1.

3 Results and discussion

3.1 Synthesis and evaluation of (S)-ofloxacin-imprinted particles

3.1.1 Choice of porogens

PS has been shown [16] to be effective as crowding agents for enhancing retention of MIP sorbents in bulk polymerization, in which chloroform was adopted as the solvent. However, chloroform-PS failed to prepare microparticle by precipitation polymerization. Thus, new system of porogen applicable to crowding agents has to be developed to prepare MIP microparticle. In our study, it was founded that THF was a good choice. After PS was added into THF, MIP particles were synthesized in a short time (1.5–2 h). Interestingly, MIP particles were not generated in 24 h without the addition of PS, even with a prolonged reaction time.

The morphology of the MIP particles was studied by SEM. As shown in Fig. 2, the resulting particles prepared in PS-THF indicate a broader size distribution. In contrast, the particles prepared in ACN showed narrow dispersed spheres. The difference of the two microparticles may be contributed to different mechanism of particle formation and growth in two porogens.

All the particles prepared in PS-THF show low porosities (Table 1). For comparison, MIP microparticles were prepared in ACN, a conventional porogen in precipitation polymerization. Interestingly, MIP G, formed with neat ACN, showed noticeable porosity and a total surface area of 106.9 m^2/g. In contrast, MIP H, prepared with neat chloroform, only indicated a total surface area of 12.3 m^2/g. The MIP has similar physical characteristics in line with N_2 adsorption analysis of previously prepared imprinted materials with chloroform as porogen [48].

The pore size distribution curves obtained from N_2 adsorption (Fig. 3A) and desorption (Fig. 3B) for the MIPs were shown in the Fig. 2. The experimental distribution obtained from N_2 adsorption shows no maxima, indicating a very wide distribution of pore sizes of MIPs prepared in

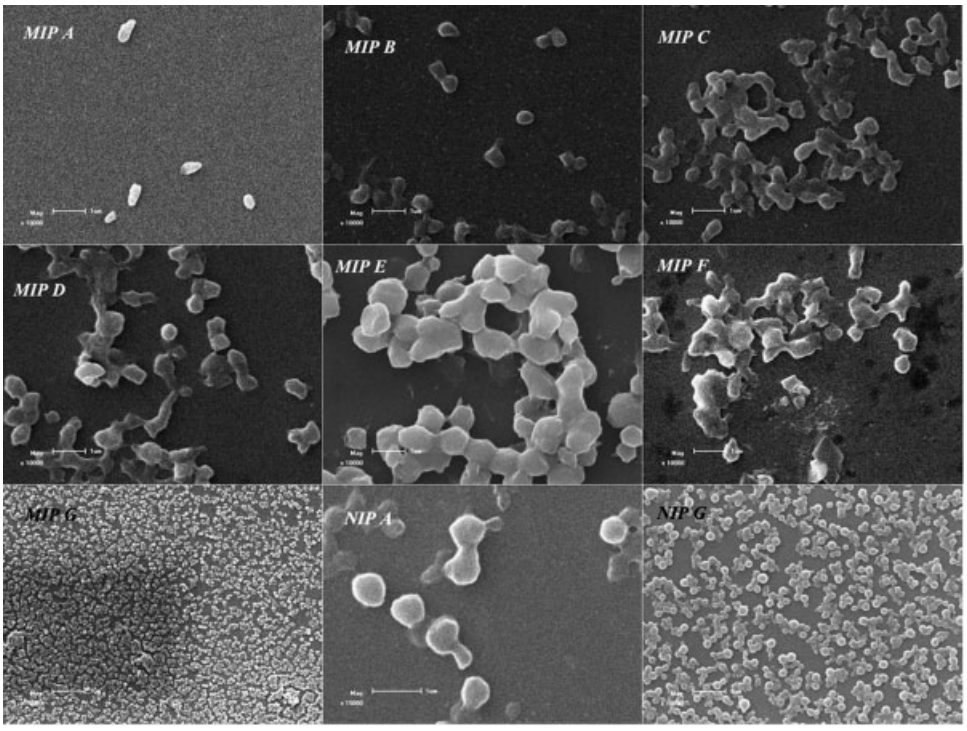

Figure 2. Scanning electron micrographs of polymeric microparticles.

PS-THF. During the adsorption process, the polymers show tangential behavior near the micropore boundary (<5 nm), with the higher surface area materials having steeper shapes in this region. Furthermore, the appearance of fine structures suggests that some pore sizes are preferred over others. For example, adsorption of MIP D almost finished in the range of 10 nm, while the adsorption process of MIP A, MIP B and MIP E were almost concentrated in the region less than 5 nm. In contrast, the experimental distribution curves obtained from desorption data is wider for the MIPs (A, B and C) than NIP A, but for MIP A, the curves show a shoulder. For the non-imprinted polymers, materials with heterogeneous pore size from the lowest mesopore limit to about 80–100 nm have been measured. The wide heterogeneous distributions of the cavity sizes, suggested by the adsorption-based plots, could be explained by formation of pre-polymerization complexes of different composition and conformation between the template molecule and the functional monomers. The appearance of just a shoulder in the case of MIP A could be explained considering the remaining part of the non-polymerized MAA monomer that interacts strongly with the template forming complexes of different composition that are washed out of the polymer during template extraction.

3.1.2 Effect of template concentration on morphology of polymer

The formation of pre-polymerization complexes affects the progression of a polymerization, thus leading to differences in the surface morphology [49]. Adjusting template amounts added to an otherwise constant pre-polymerization mixture

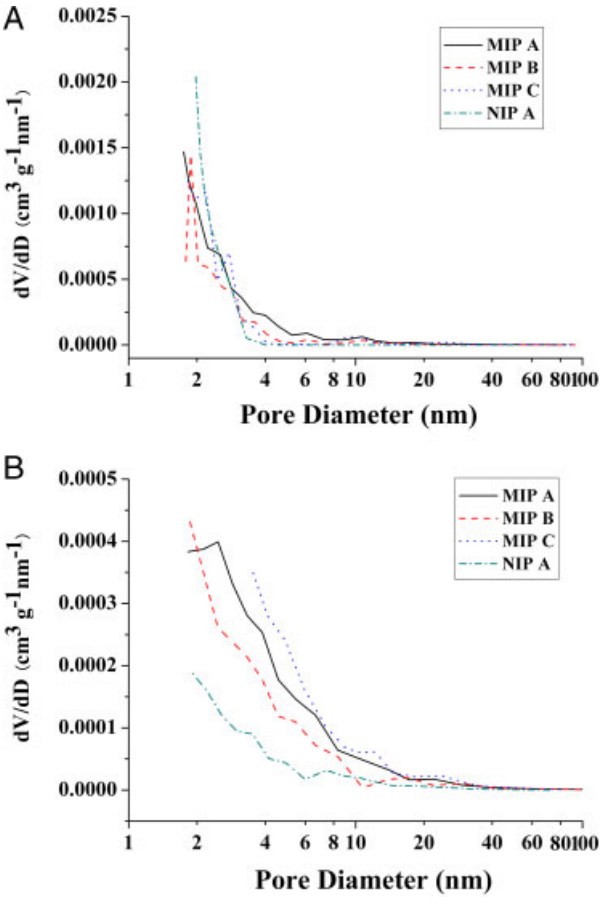

Figure 3. Barret–Joyner–Halenda (BJH) adsorption pore distribution curve (A) and BJH desorption pore distribution curve (B).

varies the molar ratio of MAA to the imprinting molecule. Different amount of template leads to different sizes of MIP particles (Table 1). For instance, the particle size of MIP A is smaller than MIP B (Fig. 2). In contrast, the particle size (MIP C) of increased template concentration runs up to 2090 nm, nearly three times larger than MIP A. In this case, the MIP particles almost cannot form a stable suspension and further evaluation in CEC is difficult.

Interestingly, the size of imprinted microparticles was about twofold of the non-imprinted references. Different from non-imprinted polymer, there is an additional molecular interaction between MAA and the template, which may affect the growth of the cross-linked MIP nuclei to result in different size of microparticles. Additionally, the surface area of microparticle increased from 2.3 to 4.8 m^2/g with increased template concentration in the pre-polymerization mixture.

We also studied the effect of the template concentration on the porous properties of resulting MIP. Table 1 indicates that when the template is introduced during polymerization, the BET area and cumulative pore volume increases. As reported by Urraca et al. [50], MIPs tend to have higher surface areas than the corresponding controls. A greater total pore volume is indicative of the MIP having a superior sample load capacity. For example, MIP A, prepared in molecular crowding agent, shows over three times the total pore volume of its corresponding control polymer (NIP A). The similar results can be found in MIPs prepared with ACN as porogen (Table 1).

3.1.3 Effect of cross-linking monomers on morphology of polymer

Three different cross-linking monomers, i.e. TRIM, DVB and EDMA, were investigated for their ability to form MIP microparticles (Table 1). Both EDMA and TRIM led to the formation of corresponding MIPs. Higher porosity of EDMA-based microparticle (MIP A, $V_p = 1.996 \times 10^{-3}\,cm^3/g$) was obtained than TRIM-based microparticle (MIP E, $V_p = 0.729 \times 10^{-3}\,cm^3/g$). Increasing or decreasing the content of TRIM resulted in larger microparticles (MIP F and MIP M) in spite of similar surface areas. When preparing MIP microparticles with DVB as the cross-linker, however, no precipitate was observed at all and only a sol fraction was isolated.

3.1.4 Influence of functional monomers on morphology of polymer

Ternary copolymers were prepared by exchanging half the amount of functional monomer, i.e. MAA, for the butyl esters of the same (BMA), AM and 4-VP. It was found that for the MIP J (Table 1) prepared with 50% of the MAA content exchanged for the AM, there was a larger MIP particle formed (> 3.6 μm). In contrast, a smaller MIP particle can be observed for the polymers prepared with BMA and 4-VP. In addition, the changes in the ratio of BMA to MAA resulted in different sizes of MIP microparticles (MIP K and L).

3.2 CEC

3.2.1 Separation conditions

A high organic content in the electrolyte has previously been shown to be optimum for MIP-based CEC separations [36]. In our work, no enantiomer separation was obtained with 80% ACN in the electrolyte. With the ACN increased to 90%, the enantiomers of ofloxacin were successfully separated. Figure 4 illustrates the separation of *rac*-ofloxacin by CEC depicting the characteristic elution order and the selective retention of the imprinted molecule as compared to the same analysis but injecting only (*S*)-ofloxacin. Increasing the ACN content further to 95% increased the EOF and resulted in the co-elution of the MIP microparticle and (*S*)-ofloxacin. The results here were in agreement with Spégel's work [33].

The effect of applied voltage on the chiral separation was also investigated. Higher voltage, i.e. 10 kV, resulted in no enantiomer separation due to co-elution of two enantiomers. However, a voltage of 5 kV provided the enantiomers separation successfully. Thus, this voltage was applied in following experiments.

The pH of the electrolyte probably provides an environment for the protonation that could affect the analyte and recognition sites of MIP [18]. In our work, the EOF increased from $1.40 \times 10^{-8}\,m^2\,V^{-1}\,s^{-1}$ at pH 3.0 to $1.92 \times 10^{-8}\,m^2V^{-1}\,s^{-1}$ at pH 7.0. MIP plug and analyte could be detected by decreasing the content of acetic acid/sodium acetate reached at 10 mmol/L. The resolution factor and the normalized separation index increased with increased pH. However, a higher pH may lead to co-elution of template with the EOF and the MIP microparticles [33]. A buffer of pH 5.0 was founded to be optimum.

The effect of the amount of MIP introduced in the capillary on the enantiomer separation was examined by varying the plug length of the MIPs, i.e. the time of the applied pressure (15 mbar). To obtain a detectable CEC separation, 2.0 s sample had to be used. Increasing the MIP plug length led to an increased elution times for two

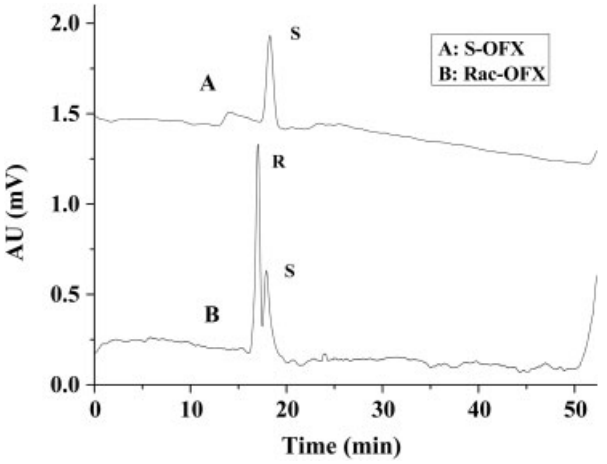

Figure 4. CEC analysis of (*S*)-ofloxacin (A) and *rac*-ofloxacin (B) demonstrating the imprinting effect and identifying the peaks.

enantiomers and improved separation. However, increasing to 6.0 s of sampling resulted in co-elution of template with EOF and MIP plug. It was founded that 4.0 s of sampling, corresponding to a MIP plug of 41% effective length (19.5 cm), was optimum. Furthermore, to obtain better chiral separation, a longer capillary, i.e. 70 cm, was used. However, such capillary resulted in an unacceptably long elution time.

3.2.2 Template to monomer ratio

In this work, the separation of the MIP B microparticles (the template to functional monomer ratio, t/m ratio, is 1/6) was lower than the MIP A with a t/m ratio of 1/4 (Fig. 5A). However, the particles with higher t/m ratio (1/3) (MIP C) showed no enantiomer selectivity. The reason for this observation could be the result of insufficient polymerization or an effect originating in morphology and porosity alterations caused by the template. As a conclusion, in view of chiral separation, optimal t/m ratio was 1/4.

3.2.3 Influence of cross-linking monomers

Two cross-linkers, EDMA and TRIM, were investigated for their ability to retain the recognition site integrity and stabilize the recognition cavity. The particles that were studied in this part had the same t/m ratio (1/4) as in MIP A. In our work, TRIM particles (MIP E) showed slightly higher resolution than EDMA particles (MIP A, Table 1). However, baseline separation was not obtained. Further increase in content of TRIM led to MIP (MIP F) (3:1) with little chiral separation, even though higher column efficiency than the MIP E. Decreasing TRIM content formed greater MIP particles; thus, it was impossible to obtain a sufficiently stable suspension for a CEC run. The binding constants and the number of binding sites have been shown to be similar for EDMA and TRIM-based MIPs [11]. The results here demonstrated the fact again.

TRIM could form the recognition cavity at relatively low degree of cross-linking [11]; thus, improved separation seemed to be the result of the relatively more open structure produced by TRIM-based MIP particles. This is supported by the fact that when there is an increase of the proportion of TRIM (Fig. 5B, MIP E and MIP F), no separation was observed. Due to stable suspensions in an electrolyte, in view of the fact above, EDMA-based microparticles were used in following experiments.

3.2.4 Functional monomer composition

Combinations of two or more functional monomers have been used to improve the recognition capabilities [51–53]. In our work, acidic functional monomers were substituted for 50% 4-VP basic functional monomer. However, no separation of *rac*-ofloxacin was found in the resulting MIP microparticle (MIP I) (Fig. 5C). Similar result was also observed with 2-VP as the co-monomer by Schweitz et al. [54]. This might be contributed to reduced quantity of hydrogen bond and the recognition sites derived from the monomer–monomer interactions. In addition, low efficiency (4700 theory plates) may be responsible for the bad separation.

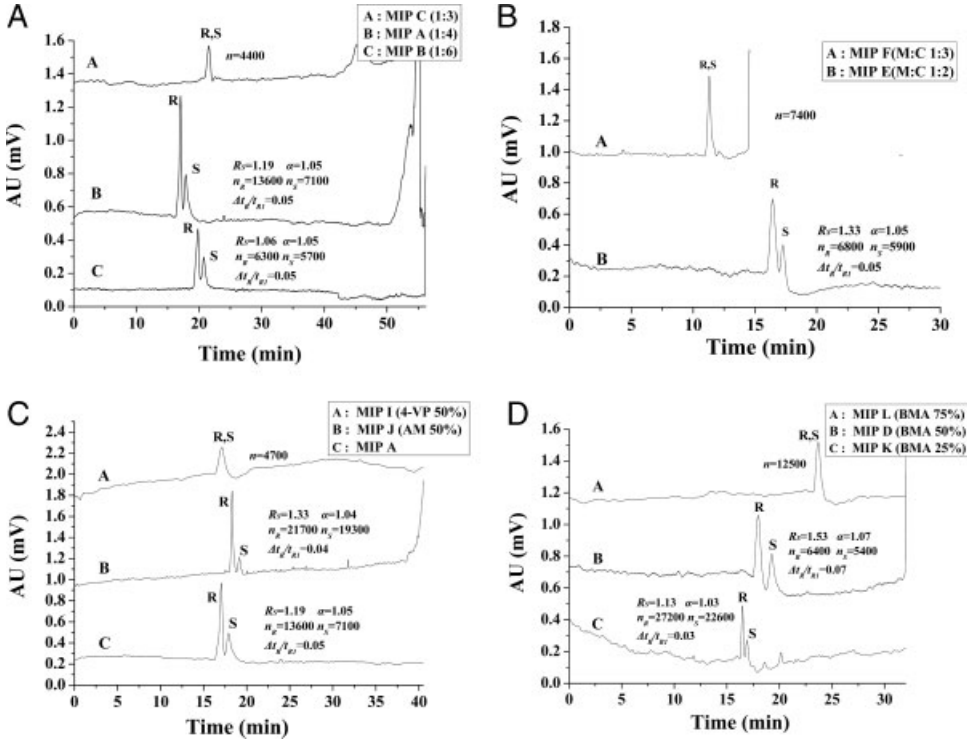

Figure 5. Polymerization variables on the recognition ability of the (*S*)-ofloxacin imprinted micro-particles. (A) Effect of template to monomer ratio: (A) MIP C (t/m 1/3); (B) MIP A (t/m 1/4); (C) MIP B (t/m 1/6). (B) Effect of the type of cross-linker: MIP E (m/c 1/2) and MIP F (m/c 1/3) prepared with TRIM. (C) Effect of combinations of two functional monomers: (A) 4-VP; (B) AM; (C) pure MAA. (D) Effect of hydrophobic co-monomer: (A) 75% BMA; (B) 50% BMA; (C) 25% BMA. The voltage was 5 kV and detection was performed at 254 nm.

It was demonstrated that AM could be an alternative monomer to MAA in some cases [52], since it can reduce nonspecific binding between monomer and template by avoiding an excess of negatively charged functionalities. In this study, AM was incorporated into the matrix of MIP with 50% substitution for MAA. Unexpectedly, the partial substitution with AM for MAA led to a decrease of selectivity ($\alpha = 1.04$), compared to MIP with pure MAA ($\alpha = 1.05$) (Fig. 5C). The increase of efficiency of template (19 300 theory plates), however, is more pronounced for AM-based MIP microparticle; thus, higher resolution ($Rs = 1.33$) was achieved in MIP J.

The influence of hydrophobic co-monomer on the performance of the MIP microparticles was also investigated. The approach to decrease of the nonselective interaction by partial substitution of a strong functional monomer for a weak functional monomer affected the MIP performance of chiral separation [55–57]. MAA was substituted for BMA from 25 to 75% in this study, compared with the pure functional monomer (MIP A). The enantiomer selectivity, in terms of a normalized separation index ($\Delta t_R/t_{R1}$), increases from 0.03 to 0.07 with increased BMA content (Fig. 5D). However, when 75% BMA was used, the enantiomer selectivity was lost (MIP L). Highest resolution and base-line separation were obtained in MIP D (Fig. 5D). Interestingly, an increase in the normalized separation index of MIP D was observed, as well as separation factor, compared with non-partial substitution MIP particle (MIP A). The reason for greater selectivity of MIP D may be the shift of equilibrium of the template reacting with functional monomers in the direction of complex formation side with the incorporation of BMA into MIP matrix. However, further increase in BMA ratio led to lower MAA content in MIP thus the decrease of enantiomer selectivity due to decreased pre-polymer complex [4].

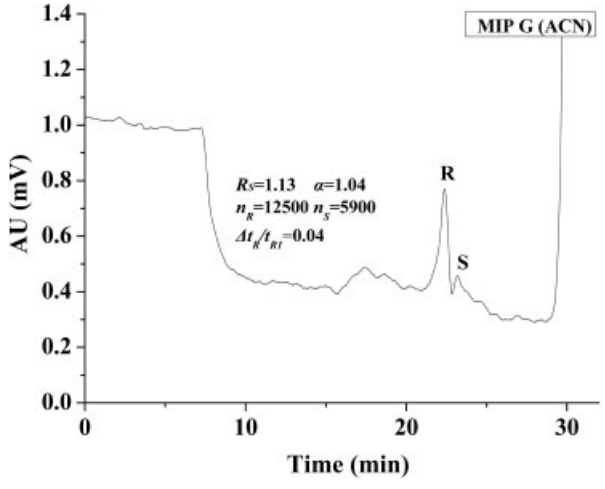

Figure 6. (S)-ofloxacin imprinted microparticles prepared with ACN. The voltage was 5 kV and detection was performed at 254 nm.

3.2.5 Influence of porogen on chiral separation

The imprinting effect of the microspheres prepared with PS-THF was also compared to that prepared with traditional porogen. Figure 6 shows the chiral separation of *rac*-ofloxacin with the microspheres prepared in ACN. Both selectivity and efficiency of the MIP microparticle were lower than with PS-THF. The increase of selectivity of PS-THF-based MIP may be the result of the function of molecular crowding in spite of identical stoichiometry used in two polymerization receipts.

The efficiency improvement from molecular crowding agent could be contributed to the alternation of morphology of MIPs. The pore size distribution of the microspheres prepared with PS-THF reveals that the pore dimensions predominantly cluster at 3 nm (35%). In comparison, the pore size distribution of the polymers prepared with ACN shows higher portion (42%) at about 20 nm. As shown in Table 1, the total pore volume of the polymers prepared with ACN is higher than PS-THF. In addition, the formers have much more pores in the range of 8–20 nm. To have strong retention and good peak shape in chromatography, the pore size in the range of 100–180 Å is usually chosen for the separation, suggesting microparticles prepared with PS-THF is more suitable to use as stationary phase than with ACN.

4 Concluding remarks

We have successfully prepared the MIP microparticles by the precipitation polymerization with a porogen system of PS-THF providing molecular crowding surrounding. Compared with traditional MIP prepared with ACN, the new MIP reported here indicated higher selectivity and efficiency. Template to functional monomer ratios of 1/4 was the optimal ratio in terms of the performance of chiral separation. The partial substitution with weaker functional monomers, BMA, for MAA increased separation efficiency and base-line separation of *rac*-ofloxacin can be achieved. In addition, EDMA-based and TRIM-based MIPs microparticles indicated comparable separation ability. Further work should consider exploring effective crowding agents and/or good solvents to obtain monodisperse nanoparticle.

This work was supported by the National Natural Science Foundation of China (Grant No. 21075090) and the Natural Science Foundation of Tianjin (No. 08JCYBJC02000).

The authors have declared no conflict of interest.

5 References

[1] Wulff, G., *Angew. Chem. Int. Ed. Engl.* 1995, *34*, 1812–1832.

[2] Tokonami, S., Shiigi, H., Nagaoka, T., *Anal. Chim. Acta* 2009, *641*, 7–13.

[3] Haupt, K., *Anal. Chem.* 2003, *75*, 376A–383A.

[4] Wulff, G., *Chem. Rev.* 2002, *210*, 1–27.

[5] Ye, L., Haupt, K., *Anal. Bioanal. Chem.* 2004, *378*, 1887–1897.

[6] Turiel, E., Martin-Esteban, A., *J. Sep. Sci.* 2009, *32*, 3278–3284.

[7] Cunliffe, D., Kirby, A., Alexander, C., *Adv. Drug Deliv. Rev.* 2005, *57*, 1836–1853.

[8] Haginaka, J., *J. Sep. Sci.* 2009, *32*, 1548–1565.

[9] Nantasenamat, C., Isarankura-Na-Ayudhya, C., Naenna, T., Prachayasittikul, V., *Biosens. Bioelectron.* 2007, *22*, 3309–3317.

[10] Sellergren, B., *Makromol. Chem.* 1989, *190*, 2703–2711.

[11] Yu, C., Mosbach, K., *J. Chromatogr. A* 2000, *888*, 63–73.

[12] Sellergren, B., Dauwe, C., Schneider, T., *Macromolecules* 1997, *30*, 2454–2459.

[13] Minton, A. P., *J. Biol. Chem.* 2001, *276*, 10577–10580.

[14] Miyoshi, D., Matsumura, S., Nakano, S., Sugimoto, N., *J. Am. Chem. Soc.* 2004, *126*, 165–169.

[15] Nakano, S., Karimata, H., Ohmichi, T., Kawakami, J., Sugimoto, N., *J. Am. Chem. Soc.* 2004, *126*, 14330–14331.

[16] Matsui, J., Goji, S., Murashima, T., Miyoshi, D., Komai, S., Shigeyasu, A., Kushida, T., Miyazawa, T., Yamada, T., Tamaki, K., Sugimoto, N., *Anal. Chem.* 2007, *79*, 1749–1757.

[17] Nilsson, C., Birnbaum, S., Nilsson, S., *J. Chromatogr. A* 2007, *1168*, 212–224.

[18] Schweitz, L., Spegel, P., Nilsson, S., *Electrophoresis* 2001, *22*, 4053–4063.

[19] Liu, Z.-S., Zheng, C., Yan, C., Gao, R.-Y., *Electrophoresis* 2007, *28*, 127–136.

[20] Huang, Y.-P., Liu, Z.-S., Zheng, C., Gao, R.-Y., *Electrophoresis* 2009, *30*, 155–162.

[21] Schweitz, L., Andersson, L. I., Nilsson, S., *Anal. Chem.* 1997, *69*, 1179–1183.

[22] Cacho, C., Schweitz, L., Turiel, E., Perez-Conde, C., *J. Chromatogr. A* 2008, *1179*, 216–223.

[23] Li, M., Lin, X., Xie, Z., *J. Chromatogr. A* 2009, *1216*, 5320–5326.

[24] Wu, X., Wei, Z.-H., Huang, Y.-P., Liu, Z.-S., *Chromatographia* 2010, *72*, 101–109.

[25] Schweitz, L., *Anal. Chem.* 2002, *74*, 1192–1196.

[26] Huang, Y.-C., Lin, C.-C., Liu, C.-Y., *Electrophoresis* 2004, *25*, 554–561.

[27] Zaidi, S. A., Cheong, W. J., *J. Chromatogr. A* 2009, *1216*, 2947–2952.

[28] Lin, J. -M., Uchiyama, K., Hobo, T., *Chromatographia* 1998, *47*, 625–629.

[29] Chirica, G., Remcho, V. T., *Electrophoresis* 1999, *20*, 50–56.

[30] Quaglia, M., De Lorenzi, E., Sulitzky, C., Caccialanza, G., Sellergren, B., *Electrophoresis* 2003, *24*, 952–957.

[31] Walshe, M., Garcia, E., Howarth, J., Smyth, M. R., Kelly, M. T., *Anal. Commun.* 1997, *34*, 119–121.

[32] Schweitz, L., Spégel, P., Nilsson, S., *Analyst* 2000, *125*, 1899–1901.

[33] Spégel, P., Schweitz, L., Nilsson, S., *Electrophoresis* 2001, *22*, 3833–3841.

[34] Spégel, P., Nilsson, S., *Am. Lab.* 2002, *34*, 29–33.

[35] Spégel, P., Schweitz, L., Nilsson, S., *Anal. Chem.* 2003, *75*, 6608–6613.

[36] de Boer, T., Mol, R., de Zeeuw, R. A., de Jong, G. J., Sherrington, D. C., Cormack, P. A. G., Ensing, K., *Electrophoresis* 2002, *23*, 1296–1300.

[37] Priego-Capote, F., Ye, L., Shakil, S., Shamsi, S. A., Nilsson, S., *Anal. Chem.* 2008, *80*, 2881–2887.

[38] Ye, L., Cormack, P. A. G., Mosbach, K., *Anal. Commun.* 1999, *36*, 35–38.

[39] Zaidi, S. A., Han, K. M., Kim, S. S., Hwang, D. G., Cheong, W. J., *J. Sep. Sci.* 2009, *32*, 996–1001.

[40] Yan, H., Row, K. H., *Anal. Chim. Acta* 2007, *584*, 160–165.

[41] Tian, M., Row, H. S., Row, K. H., *Monatsh. Chem.* 2010, *141*, 285–290.

[42] Qu, P., Lei, J., Zhang, L., Ouyang, R., Ju, H., *J. Chromatogr. A* 2010, *1217*, 6115–6121.

[43] Zhou, S., Ouyang, J., Baeyens, W. R. G., Zhao, H., Yang, Y., *J. Chromatogr. A* 2006, *1130*, 296–301.

[44] Awadallah, B., Schmidt, P. C., Wahl, M. A., *J. Chromatogr. A* 2003, *988*, 135–143.

[45] Zeng, S., Zhong, J., Pan, L., Li, Y., *J. Chromatogr. B* 1999, *728*, 151–155.

[46] Zaidi, S. A., Han, K. M., Hwang, D. G., Cheong, W. J., *Electrophoresis* 2010, *31*, 1019–1028.

[47] Liu, Z.-S., Xu, Y.-L., Yan, C., Gao, R.-Y., *J. Chromatogr. A* 2005, *1087*, 20–28.

[48] Sellergren, B., Shea, K. J., *J. Chromatogr. A* 1993, *635*, 31–49.

[49] O'Mahony, J., Molinelli, A., Nolan, K., Smyth, M. R., Mizaikoff, B., *Biosens. Bioelectron.* 2006, *21*, 1383–1392.

[50] Urraca, J. L., Carbajo, M. C., Torralvo, M. J., González-Vázquez, J., Orellana, G., Moreno-Bondi, M. C., *Biosens. Bioelectron.* 2008, *24*, 155–161.

[51] Lin, J.-M., Nakagama, T., Uchiyama, K., Hobo, T., *J. Phamaceut. Biomed. Anal.* 1997, *15*, 1351–1358.

[52] Yu, C., Mosbach, K., *J. Org. Chem.* 1997, *62*, 4057–4064.

[53] Zhang, S.-J., Huang, Y.-P., Liu, Z.-S., Duan, H.-Q., *Polym. Adv. Technol.* 2011, *22*, 286–292.

[54] Schweitz, L., Andersson, L. I., Nilsson, S., *J. Chromatogr. A* 1997, *792*, 401–409.

[55] Schweitz, L., Andersson, L. I., Nilsson, S., *Analyst* 2002, *127*, 22–28.

[56] Li, Z. Y., Liu, Z. S., Zhang, Q. W., Duan, H. Q., *Chin. Chem. Lett.* 2007, *18*, 322–324.

[57] Huang, Y.-P., Zhang, S.-J., Wu, X., Zhang, Q.-W., Liu, Z.-S., *Chromatographia* 2009, *70*, 691–698.

